Cellular/Molecular

TAG1 Regulates the Endocytic Trafficking and Signaling of the Semaphorin3A Receptor Complex

Puneet Dang, Elizabeth Smythe, and Andrew J. W. Furley

Centre for Membrane Interactions and Dynamics, Department of Biomedical Science, University of Sheffield, Western Bank, Sheffield S10 2TN, United Kingdom

Endocytic trafficking of membrane proteins is essential for neuronal structure and function. We show that Transient Axonal Glycoprotein 1 (TAG1 or CNTN2), a contactin-related adhesion molecule, plays a central role in the differential trafficking of components of the semaphorin3A (Sema3A) receptor complex into distinct endosomal compartments in murine spinal sensory neuron growth cones. The semaphorin3A receptor is composed of Neuropilin1 (NRP1), PlexinA4, and L1, with NRP1 being the ligand-binding component. TAG1 interacts with NRP1, causing a change in its association with L1 in the Sema3A response such that L1 is lost from the complex following Sema3A binding. Initially, however, L1 and NRP1 endocytose together and only become separated intracellularly, with NRP1 becoming associated with endosomes enriched in lipid rafts and colocalizing with TAG1 and PlexinA4. When TAG1 is missing, NRP1 and L1 fail to separate and NRP1 does not become raft associated; colocalization with PlexinA4 is reduced and Plexin signaling is not initiated. These observations identify a novel role for TAG1 in modulating the intracellular sorting of signaling receptor complexes.

Introduction

Trafficking of membrane proteins is critically important to neuronal development and function (Sheen et al. 2004; Lowe, 2005; Lee and Gao, 2008; Collinet et al., 2010; Kawauchi et al., 2010). Endocytosis clears receptors from the cell surface and the endocytic route followed by receptors affects receptor signaling, turnover, and recycling (Di Guglielmo et al., 2003; Sorkin and von Zastrow, 2009), thus enabling essential processes such as desensitization and adaptation.

Much is known of the intracellular components that exist to control trafficking pathways (Conner and Schmid, 2003), but how membrane receptor composition affects pathway selection is less well studied. The transmembrane protein Neuropilin1 (NRP1) is the ligand-binding component of receptor complexes for distinct families of extracellular ligands, class 3 semaphorins (Sema3A–F), and vascular endothelial growth factors (VEGF-A–E) (Tran et al., 2007; Pellet-Many et al., 2008). In endothelial cells, NRP1 signaling stimulated by Sema3s is distinct from that stimulated by VEGFs (Pellet-Many et al., 2008) due to the association of NRP1 with different coreceptor partners, Plexins and VEGF receptors, respectively (Pellet-Many et al. 2008). These associations lead to internalization of NRP1 via different endocytic pathways (Salikhova et al., 2008).

However, Sema3A can evoke distinct responses from different classes of cortical neurons, even when they express the same receptor complex components: NRP1, PlexinA4, and L1 (Castellani et al., 2000, 2002; Carcea et al., 2010). This appears to be because responsive neurons internalize Sema3A via a lipid raft-mediated, rather than clathrin-mediated endocytic pathway (Carcea et al., 2010). However, since both L1 and PlexinAs have been shown to promote clathrin-mediated NRP1 endocytosis (Castellani et al., 2004), the mechanism controlling this differential trafficking remains unclear.

Embryonic spinal sensory afferents also show differential responsiveness to Sema3A (Messersmith et al., 1995; Püschel et al., 1996; Fu et al., 2000; Pond et al., 2002), which correlates with expression of the glycosylphosphatidylinositol (GPI)-linked, L1-related molecule Transient Axonal Glycoprotein 1 (TAG1). Loss of TAG1 results in premature entry of presumptive nociceptive fibers into the dorsal horn and loss of their response to Sema3A *in vitro* (Law et al., 2008). Sensory growth cones lacking TAG1 fail to clear NRP1 and L1 from their surfaces after Sema3A treatment, suggesting that TAG1 may be required for endocytosis of the Sema3A receptor complex (Law et al., 2008).

Here we show that TAG1 interacts directly with NRP1 and can be found complexed with L1 and NRP1 at the cell surface. We demonstrate that TAG1 is required for several events that occur after Sema3A treatment, including increased association of NRP1 with PlexinA4 and stimulation of clathrin-mediated endocytosis of L1. However, we find that although L1 and NRP1 are endocytosed together after Sema3A treatment, L1 dissociates from the receptor complex and is trafficked in a pathway distinct from NRP1, which instead colocalizes with TAG1 and PlexinA4. Con-

Received Nov. 24, 2011; revised May 2, 2012; accepted June 1, 2012.

Author contributions: P.D., E.S., and A.J.W.F. designed research; P.D. performed research; P.D., E.S., and A.J.W.F. analyzed data; P.D., E.S., and A.J.W.F. wrote the paper.

This work was supported by a University of Sheffield studentship and a Wellcome Trust VIP Award to P.D. and grants to A.J.W.F. from the Biotechnology and Biological Sciences Research Council (BBSRC). We thank D. Felsenfeld, Y. Goshima, T. Jessell, S. Kenwrick, A. Kolodkin, V. Lemmon, H. Fujisawa, A. Püschel, F. Rathjen, L. Reichardt, M. Tessier-Lavigne, and A. Yaron for reagents. We also thank the University of Sheffield Light Microscopy Facility (Wellcome Grant GR077544AIA) and M. Placzek for microscopy facilities. Our thanks to an anonymous reviewer for suggesting a significant restructuring of the paper.

Correspondence should be addressed to Andrew J. W. Furley at the above address. E-mail: a.j.furley@sheffield.ac.uk.

P. Dang's present address: Perelman School of Medicine, University of Pennsylvania, Philadelphia, PA 19104.

DOI:10.1523/JNEUROSCI.5874-11.2012

 0270-6474/12/3210370-13$15.00/0

sistently, this separation does not occur when TAG1 is missing and phosphorylation of CRMP2, an early indication of Sema3A signaling (Uchida et al., 2005), does not occur. Thus, TAG1 has a critical role in trafficking NRP1 and L1 into distinct endocytic pathways, which appears necessary for Sema3A signal generation.

Materials and Methods

Animals

Maintenance of TAG1 null mutant mice on C57BL/6 background was as reported (Poliak et al., 2003). Animals were maintained with appropriate UK Home Office and Local Ethical Committee approval.

Antibodies and reagents

Antibodies used were as reported (Law et al., 2008) with the addition of anti-TAG1 polyclonal (from I. Horresh and E. Peles, Weizmann Institute of Science, Rehovot, Israel), L1-ICD and 74-5H7 mAb (from V. Lemmon, University of Miami, Miami, FL), pCRMP (from Y. Goshima, Yokohama City University, Yokohama, Japan), and PlexinA4 (from H. Fujisawa, Nagoya University Graduate School of Science, Nagoya, Japan). L1 Fab fragment was prepared from L1–324 by Bioserv UK Ltd.

DNA expression constructs as reported (Law et al., 2008) with the addition of full-length FLAG-tagged NRP1 (from A. Kolodkin, Johns Hopkins University School of Medicine, Baltimore, MD; Kolodkin et al., 1997). Sema3A protein was produced by transfection of Sema3A in COS7 cells as described by Law et al. (2008). Alexa Fluor-555 CTxB was purchased from Invitrogen.

Culture, manipulation, and immunoanalysis of dorsal root ganglion neurons

Dissected dorsal root ganglia (DRGs) from embryonic day 13.5 embryos of either sex were cultured on PDL-coated coverslips in Opti-MEM supplemented with 50 ng/ml nerve growth factor for 14–18 h and immunostaining carried out as described previously (Law et al., 2008).

Preparation of detergent-resistant membranes from growth cones. Triton X-100 extraction of soluble membranes was adapted from Guirland et al., 2004, and from cytoskeletal protein fixation methodology (Letourneau, 1983). DRG explants treated with mock or Sema3A-conditioned medium were quickly chilled and extracted in ice-cold microtubule stabilizing buffer (2 mM $MgCl_2$, 10 mM EGTA, 60 mM Pipes, pH 7.0) containing 0.1% Triton X-100 for 1 min followed by fixation with 4% paraformaldehyde (PFA) on ice and then room temperature (RT) for 15 min each, and then immunostained as above. The nonspecific total protein dye 5-(4,6-dichlorotriazin-2yl) aminofluorescein (DTAF, Sigma) was applied (0.0002% w/v) for 2 h to detect the total protein content and outline of growth cones.

Cholera toxin B labeling of lipid rafts. DRG neurons treated with mock or Sema3A-conditioned medium for 5 min were rinsed in ice-cold L15 medium followed by 1 mg/ml cholera toxin B in L-15 medium for 1 h at 12°C (Guirland et al., 2004). Cells were then rinsed 2× in PBS and fixed with 4% paraformaldehyde for 1 h at RT to fix the lipid rafts (Mayor et al., 1998), and then immunostained as above.

L1 Fab and CTxB uptake assay. The protocol for ligand endocytosis was adapted from Salikhova et al. (2008). DRG neurons in culture were cooled on ice, the medium removed, and Alexa Fluor 555-cholera toxin-B (1 mg/ml) or L1 Fab (25 mg/ml) added in fresh Opti-MEM for 20 min on ice. Cells were then rinsed in Opti-MEM and returned to warm culture medium, together with mock or Sema3A-conditioned medium and incubated at 37°C for various intervals to allow endocytosis of cholera toxin-B or L1 Fab. Then cells were placed on ice to stop endocytosis and ice-cold glycine stripping buffer (100 mM glycine, 100 mM NaCl, pH 2.5) added for 2 min to remove all surface-bound ligands. Then cells were washed 2× in ice-cold PBS, fixed with 4% PFA on ice and then at RT for 15 min each, and then immunostained as above.

Immunofluorescence microscopy

Images were acquired on an Olympus BX61 microscope with GRID confocal using Volocity software version 5.5 (Improvision) or Zeiss AxioImagerZ1 with ApoTome. A 100× UPlan Apo oil objective with a numerical aperture of 1.4 was used, and images were acquired as z-stacks with 0.2 μm spacing. This gives a voxel size of 60 nm in the *X*- and *Y*-axes and 200 nm in the *Z*-axis. Twenty images were acquired for each experimental treatment/time-point. Within an experiment, the exposure times for each fluorescence channel were kept constant in order to enable the comparison of fluorescence intensities across the various conditions.

Image analysis using Volocity

All postacquisition analysis of images was done using Volocity software (PerkinElmer). The region of growth cone used for analysis was the distal 30 μm of axon. For determination of total protein levels, the total fluorescence intensity in the region of interest was measured and the background subtracted. The average of "total" fluorescence intensity for each treatment/time point (± SEM) was used for analysis. For colocalization analyses, z-stacks were deconvolved using iterative restoration (confidence limit of 98%, maximum of 25 iterations). Thresholds were set for each channel to 20–30% of the maximum intensity and input in the colocalization function to determine the colocalization coefficient for each channel. The mean colocalization coefficient (± SEM) for each treatment/time point was used for comparison.

Compiled datasets from at least two experiments were analyzed for statistical significance in Prism software (GraphPad) using two-tailed unpaired *t* test with Welch's correction for unequal variances (two groups of data) or one-way ANOVA with Bonferroni's multiple-comparison test (more than two groups of data). Confidence interval used was set to 95%, with a p value <0.05 taken as statistically significant. The p values obtained were summarized using asterisks as $^{*}p < 0.05$, $^{**}p < 0.01$, $^{***}p < 0.001$.

Results

Sema3A induces L1 endocytosis and AP2 binding site dephosphorylation in growth cones

The endocytosis of NRP1 from the cell surface following Sema3A binding has been shown to require the presence of L1, at least in cos7 cells (Castellani et al. 2004). However, although L1 is known to be endocytosed in growth cones during L1-stimulated axon growth (Kamiguchi et al., 1998; Kamiguchi and Lemmon, 2000) and in cos7 cells after Sema3A treatment (Castellani et al. 2004), formal proof that L1 endocytosis is stimulated in growth cones after Sema3A treatment is lacking. To follow L1 endocytosis directly, Fab fragments of anti-L1 monoclonal antibody (mAb 324) were applied in cold medium to live wild-type (WT) growth cones for 10 min on ice. The cold medium was then replaced with fresh medium at 37°C, with or without Sema3A but containing no anti-L1 Fab, for different periods before fixation and visualization of internalized antibody (Kamiguchi et al., 1998). In control conditions, the fluorescence intensity due to internalized L1 Fab remained constant over 20 min (Fig. 1*A*), consistent with previous studies showing that L1 is constitutively endocytosed and recycled during axon growth (Kamiguchi and Lemmon, 2000). However, the intensity of this fluorescence increased significantly 10 min after Sema3A exposure, reflecting a large increase in the number of Fab-containing internalized particles. By 20 min the internalized particles become concentrated, usually into a single large aggregate (Fig. 1*A*, arrowhead). At the same time the overall fluorescence appeared to have fallen, suggesting that L1 may be recycled or degraded, although it is possible that saturation of the fluorescence signal caused us to underestimate the amount of L1 present in the aggregate. Such aggregation of internalized Fab was never seen in untreated growth cones.

In L1-stimulated axon growth, L1 is endocytosed via an AP-2, clathrin, and dynamin-dependent pathway (Kamiguchi et al., 1998; Kamiguchi and Yoshihara, 2001). Consistent with the idea that Sema3A-induced L1 endocytosis uses a similar pathway, we found that the colocalization of L1 with clathrin heavy chain increases 5 min after Sema3A treatment (Fig. 1*B*). The clathrin

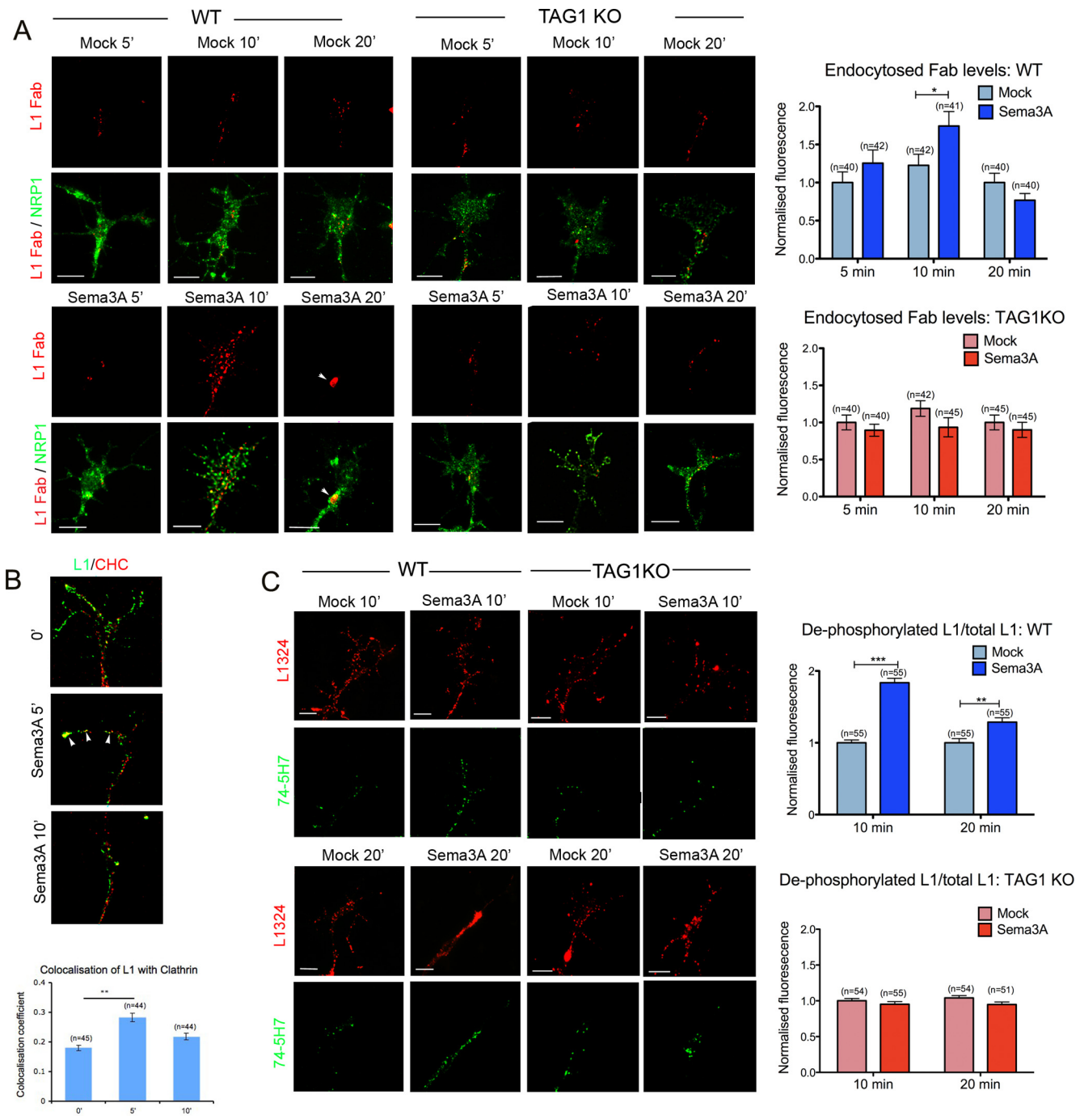

Figure 1. Sema3A treatment induces an increase in clathrin-associated L1 endocytosis ***A***, Endocytosis of L1 Fab DRG growth cones was monitored for 5, 10, or 20 minutes (') in the presence of Mock or Sema3A medium. Cells were acid stripped, fixed, permeabilized, and immunolabeled for internalized L1 Fab (red) and counter-labeled for total NRP1 (green) to reveal the growth cone structure. The amount of L1 Fab internalized following 10 min of Sema3A treatment increased significantly in WT but not TAG1 KO growth cones (one-way ANOVA, $p < 0.0001$ for WT, $p = 0.1769$ for TAG1 KO). ***B***, Growth cones treated with Sema3A for the indicated times were fixed, permeabilized, and immunolabeled for L1 (green) and clathrin heavy chain (CHC; red). Quantitation revealed that colocalization of L1 and CHC rose significantly within 5 min of Sema3A treatment. ***C***, Growth cones treated with Mock or Sema3A medium were labeled for total L1 (L1–324, red) and 74-5H7 mAb (green). The amount of fluorescence intensity detected by the 74-5H7 mAb increases upon 10 min of Sema3A treatment in WT but not TAG1KO growth cones (one-way ANOVA, $p < 0.0001$ for WT, $p = 0.1769$ for TAG1KO). Data are combined values from three independent experiments. (*n*, number of growth cones; $^{***}p < 0.001$, $^{**}p < 0.01$, $^{*}p < 0.05$, Bonferroni's multiple-comparison test). Scale bar, 5 μm.

adaptor AP-2 binds to L1 via the YRSL motif present in the cytoplasmic tail of L1, which is required for L1 endocytosis, but this binding is inhibited by phosphorylation of the leading tyrosine (Y1176; Schaefer et al., 2002). Phosphorylation of Y1176 also blocks binding of the mAb 74-5H7 (Schaefer et al., 2002). 74-5H7 immunoreactivity is found associated with L1 in endocytic vesicles and can be used to detect L1 that is available for AP-2-dependent endocytosis (Kamiguchi et al., 1998; Schaefer et al., 2002). We therefore used 74-5H7 to determine whether the enhanced L1 endocytosis seen after Sema3A treatment is likely to be AP-2 dependent. Consistent with this idea, we found that the ratio of dephosphorylated (74-5H7 immunoreactive) to total L1

(mAb 324 immunoreactive) increased almost twofold after Sema3A treatment, compared to mock-treated growth cones peaking at 10 min but still remaining significantly higher at 20 min (Fig. 1*C*). However, since mAb 324 recognizes an extracellular epitope (Itoh et al., 2004), it is also possible that the 324/74-5H7 ratio rises because the extracellular domain is cleaved (e.g., Mechtersheimer et al., 2001). That this is not the case is indicated by the fact that the ratio between 324 fluorescence and that from an antibody against the intracellular domain of L1 (L1-ICD; Nakamura et al., 2010), did not change after Sema3A treatment (data not shown).

Together, these data confirm that Sema3A induces a net increase in L1 endocytosis in growth cones that peaks around 10 min after treatment, most likely in an AP-2/clathrin-dependent manner. Moreover, the aggregation of the internalized particles 20 min after Sema3A treatment, but not in control growth cones, suggests that Sema3A signaling may change the endocytic pathway followed by L1.

L1 and NRP1 endocytose together but become separated internally

Although the data above and previous studies (Castellani et al., 2004) suggest that NRP1, through being complexed with L1, should undergo clathrin-mediated endocytosis (CME), disruption of cholesterol-rich membranes ("lipid rafts") in neurons (Guirland et al., 2004; Carcea et al., 2010), leukemic T cells (Moretti et al., 2008), and endothelial cells (Salikhova et al., 2008) inhibits NRP1-mediated signaling and, in a subset of cortical neurons, Sema3A internalization (Carcea et al., 2010). Indeed, growth cone responses to a range of guidance cues, both attractive and repellant, have been shown to be dependent upon the integrity of lipid rafts, and receptors for the relevant cues, including NRP1, are known to translocate to cholesterol-enriched membrane fractions during the response (Guirland et al., 2004; Marquardt et al. 2005). Together, these results have been interpreted to indicate that the Sema3A receptor complex undergoes lipid raft-mediated endocytosis (RME) in neurons that collapse in response to Sema3A (Carcea et al., 2010). However, these studies largely depended on pharmacological endocytic inhibitors, the specificity of which is controversial (Ivanov 2008), and focused on the fate of internalized NRP1 at late (e.g., 30 min) time points or on the copatching of NRP1 with lipid rafts on the cell surface (Guirland et al., 2004) and did not directly address the association of NRP1 with endocytosed L1.

Since, NRP1 has been observed to disappear from the surface of *Xenopus* retinal growth cones within 5 min of Sema3A treatment (Piper et al., 2005), we determined whether this is also true of mouse DRG growth cones. Levels of surface NRP1 dropped to less than half that of control growth cones within 5 min of treatment and remained at low levels until at least 10 min after (Fig. 2*A*), most likely remaining low until at least 45 min after treatment (Fournier et al., 2000; Law et al., 2008). Thus, like L1, NRP1 also rapidly disappears from the growth cone surface after Sema3A treatment.

To test directly whether NRP1 endocytosis with L1 increases after Sema3A treatment, we followed the colocalization of NRP1 with internalized L1 using anti-L1 Fabs as above. Five minutes after Sema3A addition, >30% of internalized Fab could be found colocalized with NRP1, a twofold increase over control (Fig. 2*B*). Strikingly, however, by 10 min this colocalization reduced to control levels and by 20 min <15% of internalized Fab could be found associated with NRP1, despite the fact that overall levels of internalized anti-L1 Fab rise over the same period (Fig. 1*A*). Because these experiments follow the fate of a single pulse of internalized anti-L1 Fab, this suggests that NRP1 initially internalizes with L1, but at later stages the molecules become separated inside the cell.

Neuropilin1 becomes enriched in CTxB-binding vesicles after Sema3A-induced endocytosis

The observation that NRP1 initially endocytoses with L1 and that Sema3A-induced L1 endocytosis appears to be clathrin dependent was unexpected, given that disruption of lipid rafts blocks responses to Sema3A (Guirland et al., 2004; Carcea et al., 2010). One possibility is that, despite the increased colocalization of L1 with clathrin and the dephosphorylation of the AP-2 binding site, in this instance NRP1 associated with L1 undergoes RME, as has been suggested (Carcea et al., 2010).

We attempted to address the endocytic route taken using classical CME and RME inhibitors [monodansylcadaverine (MDC) and filipin, respectively] but found that the inhibitors alone induced a severe reduction of NRP1 cell surface expression on control growth cones (Fig. 3*A*), suggesting that the drugs affect the steady-state recycling or export of NRP1 to the cell surface and precluding their use in the study of Sema3A-induced endocytosis.

Instead, we therefore addressed whether NRP1 becomes endocytosed with rafts after Sema3A treatment by labeling cells with uncrosslinked Alexa Fluor 555-tagged cholera toxin B subunit (CTxB), which binds raft-associated G_{M1} gangliosides (Harder et al., 1998), and followed the association of NRP1 with internalized CTxB in a manner similar to the anti-L1 Fab experiments above. In control growth cones, many CTxB-positive endocytic vesicles were found also to label for NRP1 (Fig. 3*B*), indicating that as much as 25% of total NRP1 protein undergoes RME in control conditions. However, after 5 min of Sema3A treatment, the colocalization between NRP1 and CTxB dropped to ~18%, significantly lower than control growth cones at the same stage ($p < 0.05$, unpaired *t* test). Following this initial decrease, colocalization of CTxB and NRP1 then rose to 31% at 10 min and 34% at 20 min, whereas control levels remained constant ($p < 0.05$, unpaired *t* test). Because this experiment follows the fate of a single pulse of internalized CTxB, this suggests that, in response to Sema3A, NRP1 is not initially internalized with CTxB but subsequently becomes associated with vesicles containing internalized CTxB, presumably bound to raft-associated G_{M1} gangliosides. Since the initial decrease in NRP1 colocalization with endocytic CTxB occurs coincident with the disappearance of NRP1 from the cell surface (Fig. 2*A*) and an increase in overall CTxB uptake (Fig. 3*C*), this strongly suggests that a large proportion of the endocytosis of NRP1 that occurs after Sema3A treatment does so in membranes that do not bind CTxB.

Taken together, these observations indicate that the association of NRP1 with endocytosed L1 after Sema3A treatment is inversely related to its association with endocytosed CTxB and are consistent with the idea that NRP1 is initially endocytosed with L1 in non-CTxB binding vesicles; but by 10 min the two proteins separate, and NRP1 is trafficked into intracellular compartments enriched in CTxB binding sites.

Translocation of NRP1 to CTxB-binding vesicles is TAG1 dependent

Previously, we showed that the disappearance of L1 and NRP1 from the surface of neuronal growth cones after Sema3A exposure is TAG1 dependent. To determine whether loss of TAG1 affects the early or late phase of NRP1 trafficking described above, we repeated the experiments that follow NRP1 colocalization

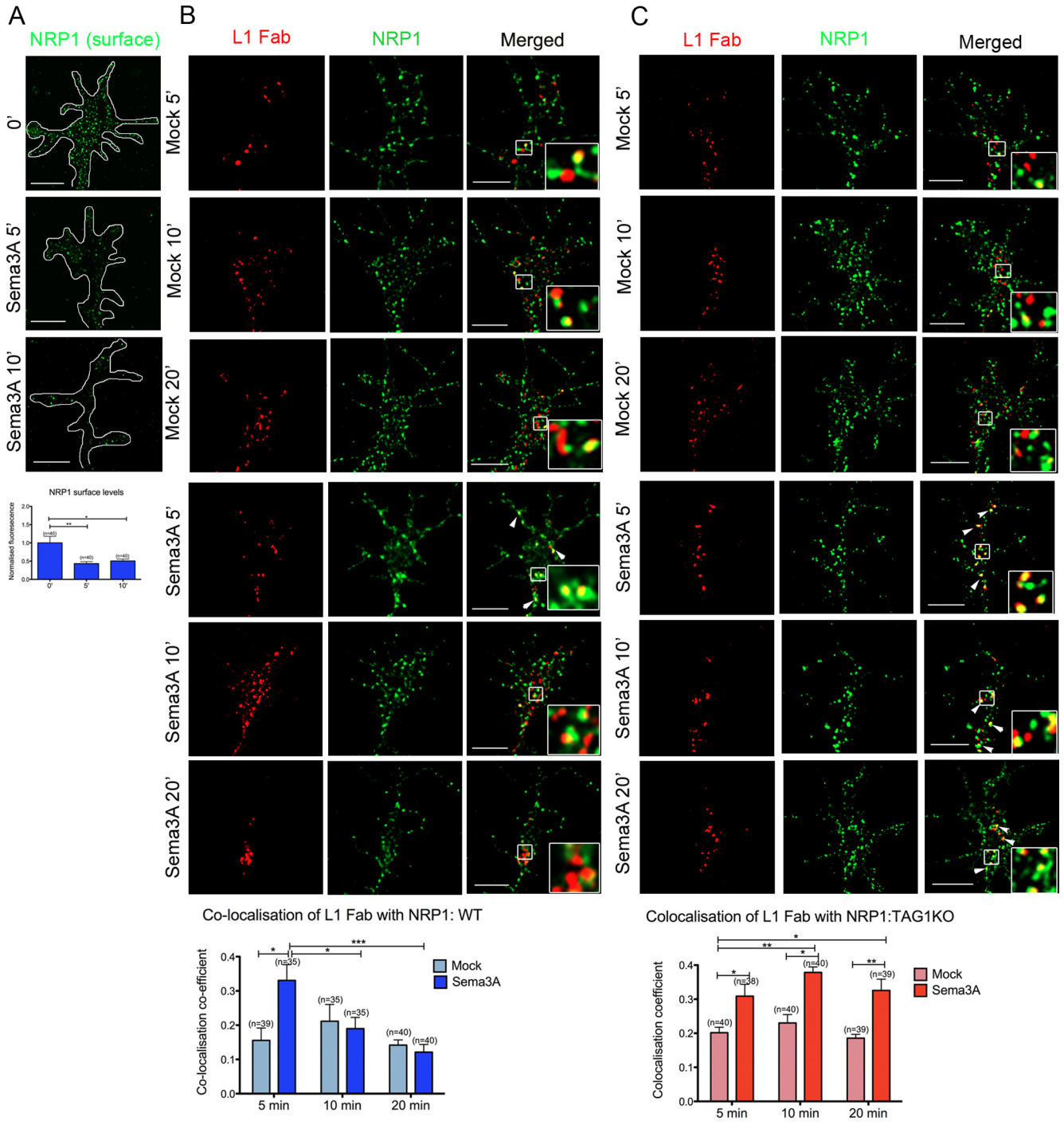

Figure 2. TAG1 is required for postendocytic separation of NRP1 from L1. ***A***, Growth cones were treated with Sema3A for the indicated times and fixed in 2% PFA containing 10% glucose to avoid permeabilization. Growth cones were immunolabeled for NRP1 (green) and the total fluorescence intensity was calculated using Volocity software. The amount of NRP1 on the surface of growth cones was reduced significantly after 5 min of Sema3A treatment and continued to be low at 10 min (one-way ANOVA, $p = 0.0024$, Bonferroni's multiple comparison test). ***B***, L1 Fab (red) was allowed to endocytose in the presence of Mock or Sema3A medium for the given times, and its colocalization with NRP1 (green) was examined. In WT growth cones, a large proportion of L1 Fab colocalized with NRP1 after 5 min of Sema3A treatment (arrowheads and insets). By 10 and 20 min this colocalization had dropped to control levels (one-way ANOVA, $p = 0.0009$). ***C***, In TAG1 KO growth cones there was a similar increase in the colocalization of L1 Fab with NRP1 after 5 min of Sema3A treatment, but this continued to remain high after 10 and 20 min of Sema3A treatment (one-way ANOVA, $p < 0.0001$) Data are combined values from two independent experiments. (*n*, number of growth cones; $^{***}p < 0.001$, $^{**}p < 0.01$, $^{*}p < 0.05$. Scale bar, 5 μm.

with internalized anti-L1 Fab or with internalized CTxB on growth cones from DRG from TAG1 knockout (TAG1KO) mice. Remarkably, although as in WT there was an initial increase in colocalization of L1 Fab with NRP1, instead of falling with time, in the absence of TAG1 colocalization was sustained for at least 20 min after Sema3A treatment with up to 38% of internalized Fab being colocalized with NRP1 at 10 min, compared to just 20% in controls (Fig. 2*C*). When we instead followed the colocalization of endocytic CTxB with NRP1, we found that the increase in the association of NRP1 with internalized CTxB that occurs in WT growth cones after 10 min (Fig. 3*B*) does not occur in TAG1KO growth cones (Fig. 3*D*). Thus, these data support the idea that

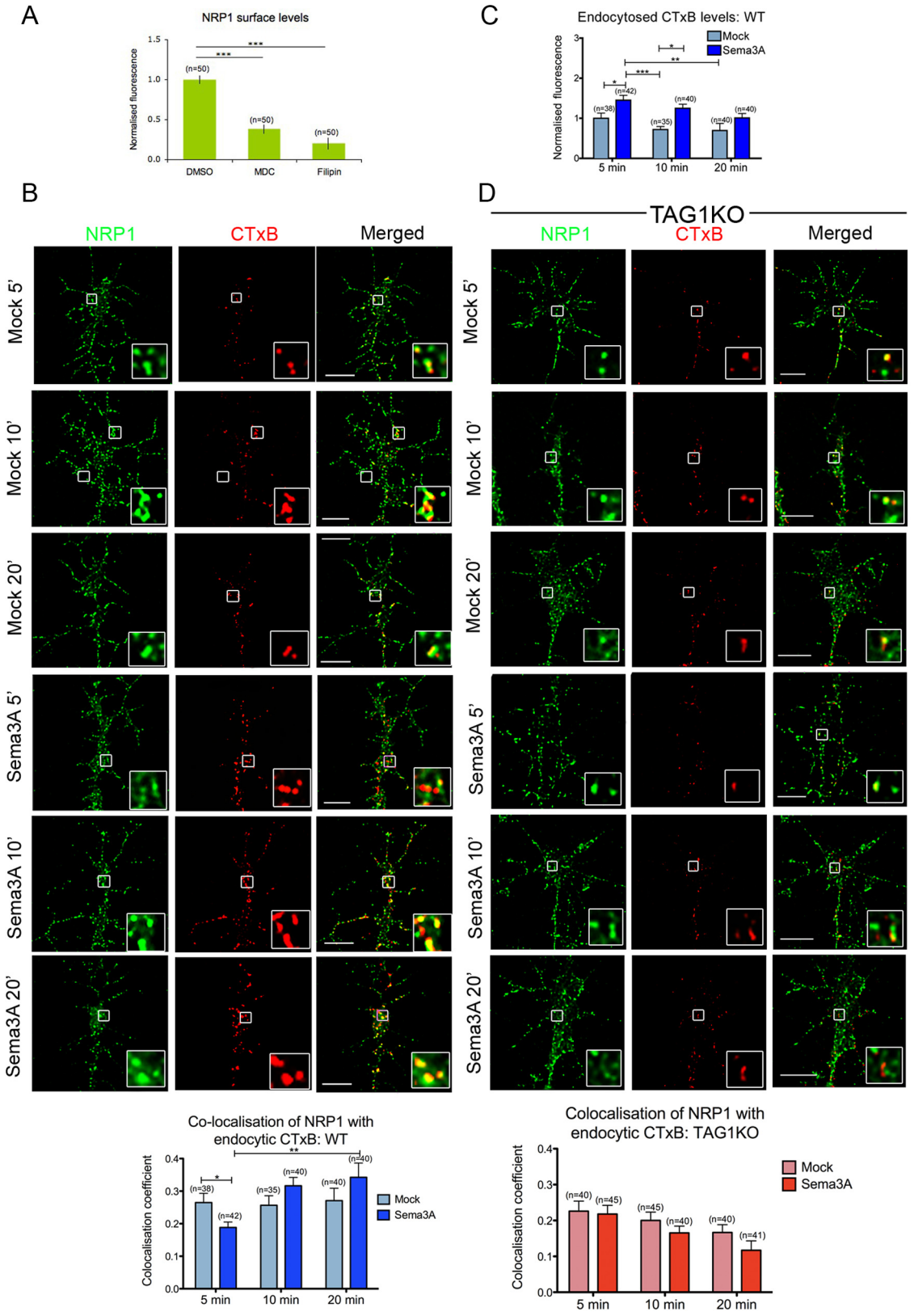

Figure 3. NRP1 is not endocytosed with CTxB after Sema3A treatment but is subsequently enriched in CTxB-positive vesicles in a TAG1-dependent manner. ***A***, Steady-state surface levels of NRP1 were examined in growth cones incubated with MDC (100 μM), filipin (1 μg/ml), or DMSO for 20 min. Both MDC and filipin caused a dramatic loss of NRP1 from the surface (one-way ANOVA, $p < 0.0001$) even though Sema3A was not added. ***B***, CTxB was allowed to endocytose similarly as L1 Fab above (Fig. 1), and its colocalization with NRP1 was examined. NRP1 colocalized with endocytic CTxB in Mock conditions. Upon Sema3A treatment, this colocalization dropped after 5 min ($p < 0.05$, Bonferroni's multiple-comparison test) but returned to control levels after 10 and 20 min, suggesting a late enrichment of NRP1 in CTxB-positive vesicles. ***C***, Graph showing that the total amount of CTxB internalized after Sema3A treatment rose significantly after 5 min, compared to mock-treatment (one-way ANOVA, $^{*}p < 0.05$), at the same time that colocalization with NRP1 falls (***B***, above). ***D***, In TAG1KO growth cones, no changes in the colocalization of NRP1 with endocytic CTxB was seen at 5 and 10 min of Sema3A treatment, while a slight drop in colocalization occurred after 20 min (one-way ANOVA, $p = 0.0361$). Data are combined values from three independent experiments (*n*, number of growth cones; $^{***}p < 0.001$, $^{**}p < 0.01$, $^{*}p < 0.05$). Scale bar, 5 μm.

TAG1 is required for the separation of NRP1 from L1 and the accompanying translocation of NRP1 to CTxB-binding vesicles, rather than the initial endocytosis of the complex from the cell surface.

TAG1 colocalization with NRP1 increases after Sema3A binding

The involvement of TAG1 in the translocation of NRP1 to CTxB-binding vesicles led us to consider how TAG1 might affect the Sema3A receptor complex. In principle, TAG1 could exert its influence through its interactions with L1 (Buchstaller et al., 1996; Rader et al., 1996; Malhotra et al., 1998). However, the known association of TAG1 with G_{M1} gangliosides (Kasahara et al., 2002; Loberto et al., 2003) led us to explore whether TAG1 might play a role in NRP1 translocation through more direct interactions with NRP1.

To understand better the relationship between the three molecules, triple labeling experiments were performed on permeabilized wild-type growth cones before and after Sema3A treatment (Fig. 4*A*). On untreated growth cones, TAG1 shows the most restricted localization and appears largely to be localized to the periphery of the growth cone, most notably on filopodia (Fig. 4*A*, arrowheads). Quantitation indicates that overall only ~5% of NRP1 and 15% of L1 is associated with TAG1. However, in the peripheral regions where TAG1 is concentrated there is clear overlap with both L1 and NRP1, and ~32% of all TAG1 is L1 associated and 20% NRP1 associated. Ten minutes after Sema3A treatment, however, the association of TAG1 with NRP1 doubles, while that with L1 remains the same. At the same time, mirroring the anti-L1 Fab results above, the colocalization of L1 and NRP1 has begun to drop, and by 20 min <10% of L1 is NRP1 associated. L1 association with TAG1 also falls to almost half untreated levels, while the association of TAG1 with NRP1 has returned to the same as untreated levels. As with the internalized anti-L1 Fab experiments, after Sema3A treatment the bulk of L1 labeling is in a large aggregate; TAG1 and NRP1 labeling does not follow this pattern.

Together, the data above support that L1 becomes separated from NRP1 after Sema3A treatment, apparently entering a distinct intracellular structure. By contrast, the association of NRP1 with TAG1 increases during the course of the Sema3A response. Thus, although previously we had been unable to find evidence for an interaction of NRP1 and TAG1 in *trans* (Law et al., 2008), this raised the possibility that TAG1 and NRP1 might interact in *cis*.

Sema3A binding dissociates L1 from NRP1 in a TAG1-dependent manner

To test for interactions between TAG1 and NRP1, we coexpressed full length cDNAs for all three molecules in combinations in cos7 cells (Fig. 4*B*). As expected, immunoprecipitation of NRP1 coprecipitated L1 (Castellani et al., 2000) whether or not TAG1 was present (Fig. 4*B*, CONTROL, lanes 7 and 8, bottom panel). Surprisingly, however, NRP1 also coprecipitated TAG1, even when L1 was absent (lanes 6 and 8, middle panel). Thus, in cos7 cells, TAG1 appears to be part of the Sema3A receptor complex and to interact with NRP1 independently of L1.

Our colocalization studies suggested that the association of NRP1 with L1 might change upon Sema3A binding. To test this, we examined the associations of NRP1, L1, and TAG1 30 min after Sema3A treatment of transfected cos7 cells; previous studies have shown that these cells respond to Sema3A when transfected with appropriate NRP1 and L1 or PlexinA combinations (Takahashi et al., 1999, Zanata et al., 2002, Castellani et al., 2004). Immunoprecipitation of NRP1 from Sema3A-treated cells cotransfected with NRP1 and L1 (Fig. 4*B* Sema3A, lane 7, bottom), or NRP1 and TAG1 (lane 6, middle), coprecipitated L1 and TAG1, respectively, similar to untreated cells (Fig. 4*B*, CONTROL). However, immunoprecipitation of NRP1 from Sema3A-treated cells transfected with cDNAs for all three proteins (NRP1/L1/TAG1) only coprecipitated TAG1, not L1, which now appeared to be completely absent from the complex (Fig. 4*B*, Sema3A, lane 8, asterisks highlight comparison). Thus, Sema3A binding to NRP1 on cos7 cells results in its dissociation from L1, but only when TAG1 is present. Although earlier time points were not assayed, that NRP1 and L1 are separated 30 min after Sema3A treatment in cos cells is consistent with the observation that this separation occurs between 5 and 10 min after treatment in growth cones.

Taken together with the colocalization data from mutant and wild-type growth cones, these data indicate that TAG1 regulates the segregation of the Sema3A receptor components, NRP1 and L1, into different membrane microdomains after Sema3A binding.

L1 does not become associated with CTxB-binding membranes after Sema3A treatment

Although our observation that NRP1 is trafficked intracellularly into CTxB-binding, presumably raft-enriched membranes is consistent with previous observations that disruption of lipid-rafts blocks Sema3A-induced growth cone collapse (Guirland et al., 2004; Carcea et al., 2010), these latter studies suggested that NRP1 translocated to rafts on the cell surface. The key evidence for this was the increase, after Sema3A treatment, of NRP1 colocalization to membrane patches induced by the cross-linking of CTxB bound to the surface of live *Xenopus* retinal growth cones (Guirland et al., 2004). Indeed, using the same technique with mouse DRG growth cones, we also found that the amount of NRP1 fluorescence associated with CTxB-induced patches almost doubled after just 5 min of Sema3A treatment (Fig. 5*A*), suggesting that as much as 20% of the accessible NRP1 becomes raft associated after Sema3A treatment. To determine whether L1 also becomes raft associated in this response, as has been hypothesized (Carcea et al., 2010), we followed L1 localization in CTxB-induced patches. In contrast to NRP1, the amount of L1 associated with CTxB did not change significantly, remaining similar to control levels even after Sema3A treatment (Fig. 5*A*). To corroborate this result, we used cold detergent extraction to isolate membrane rafts *in situ* (Guirland et al., 2004). In untreated or mock-treated growth cones, little or no NRP1 remained in growth cones after extraction, whereas substantial amounts became TX100-resistant as early as 5 min after Sema3A treatment (Fig. 5*B*). Similarly low levels of L1 were found in TX100-extracted control growth cones, but by contrast these did not change after Sema3A treatment (Fig. 5*B*). Thus, whereas a significant amount of NRP1 becomes associated with CTxB-induced membrane patches after Sema3A treatment in spinal sensory neurons, consistent with previous studies, L1 does not, nor does it become enriched in TX100-resistant membranes. This latter result is consistent with L1 being endocytosed via a non-raft-associated pathway rather than via RME.

The association of NRP1 with CTxB-induced patches at the cell surface seems at odds with our internalization data. However, it is important to note that >50% of cell surface NRP1 has already internalized (Fig. 2*A*; Piper et al. 2005) by the 5 min time point at which the CTxB patching experiments were performed, suggest-

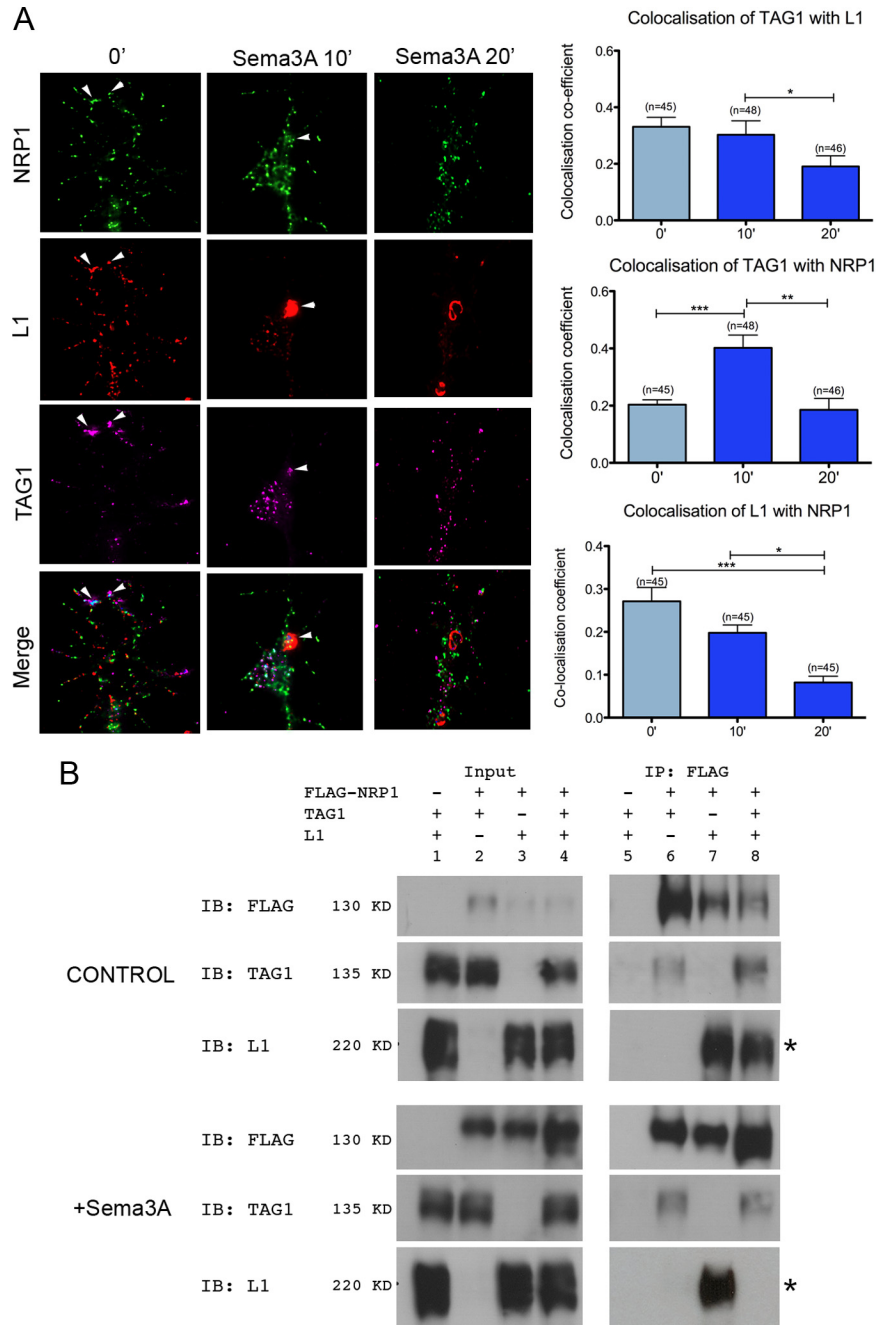

Figure 4. TAG1 is required for Sema3A-induced dissociation of L1 from the receptor complex. ***A***, Growth cones treated with Sema3A for the indicated times were fixed, permeabilized, and immunolabeled for TAG1 (purple), L1 (red), and NRP1 (green). TAG1, L1, and NRP1 were found to colocalize in untreated growth cones [0 minutes (′), arrowheads]. Some colocalization of L1 with NRP1 was still seen at 10 min (arrowheads) but was largely absent at 20 min (one-way ANOVA, $p = 0.0105$). On the other hand, colocalization of TAG1 with NRP1 increased at 10 min of Sema3A treatment and was reduced to control levels at 20 min (one-way ANOVA, $p = 0.0219$). Data are combined values from three independent experiments. (n, number of growth cones; $^{***}p < 0.001$, $^{**}p < 0.01$, $^{*}p < 0.05$, Bonferroni's test). ***B***, Cos7 cells were transfected with TAG1, L1, and NRP1 cDNA constructs in various combinations and immunoprecipitated using FLAG-M2 agarose beads against FLAG-NRP1. NRP1 interacts directly with TAG1 (lane 6) and L1 (lane 7). A complex of NRP1/TAG1/L1 can also be isolated (lane 8). In cos7 cells treated with Sema3a for 30 min (bottom panels), NRP1 still interacted with TAG1 (lane 6) and L1 (lane 7) in double-transfected cells. In triple-transfected cells the NRP1/TAG1 interaction was maintained, but not that between NRP1 and L1. Semiquantitative densitometric analysis of the bands showed that in control conditions, the following occurred: for TAG1, 29% of input protein precipitated with NRP1 when just TAG1 and NRP1 were present, compared to 39% when all three were present; for L1, 65% of input precipitated when just L1 and NRP1 were present, rising to 85% when all three were transfected. After Sema3A treatment, the following occurred: for TAG1, 20% of input precipitated when TAG1 and NRP1 were present compared to 23% with all three; for L1, 64% precipitated with NRP1 when just L1 and NRP1 were present, but this fell to just 1.8% of input when all three proteins were transfected. Scale bar, 5 μm.

ing that the raft-associated NRP1 at the cell surface may represent a separate pool. Moreover, when we assessed whether the copatching technique exclusively monitors cell surface CTxB, we in fact found that a substantial proportion of the CTxB detected was internalized (data not shown). This is perhaps not surprising, as the technique involves incubating the living cells at 12°C for 1 h after the Sema3A treatment to allow CTxB patching to occur (Guirland et al., 2004). This suggests that the pool of cell surface CTxB-associated NRP1 may be even smaller than these experiments suggest. Consistently, as for the association of NRP1 with internalized CTxB, copatching of NRP1 with CTxB was also TAG1 dependent (Fig. 5*A*), as was the enrichment of NRP1 in TX100-resistant membranes (Fig. 5*B*). Thus, either there are two pools of CTxB-associated NRP1, or these experiments in fact identify internalized NRP1 that has already started to become CTxB associated via the route described above.

Neuropilin1 associates with PlexinA4, not L1 after Sema3A treatment

The trafficking of NRP1 away from L1 after Sema3A treatment raises the important question of how this is involved in Sema3A signaling. Although NRP1 is considered to be the key ligand-binding component of the Sema3A holoreceptor complex, PlexinA4 is thought to be the main signal-generating component and is essential for Sema3A responses in DRG neurons (Suto et al. 2005; Yaron et al., 2005). Critical questions, therefore, are whether PlexinA4 is trafficked similarly to NRP1 or to L1, whether its trafficking is also TAG1 dependent, and therefore whether changes in PlexinA4-generated signaling can account for the loss of Sema3A-induced repulsion seen in TAG1KO growth cones (Law et al., 2008). To address these questions, we followed the localizations of NRP1 and PlexinA4 relative to each other, and to other complex components, on growth cones fixed and permeabilized at different time points after Sema3A treatment. As shown in Figure 6*A*, as might be expected, the amount of NRP1 that is colocalized in growth cones with PlexinA4 in control conditions is relatively high (34% of detectable NRP1), confirming that these molecules form pre-existing complexes (Takahashi et al., 1999). After addition of Sema3A, the association of NRP1 with PlexinA4 increases so that ~60% of total NRP1 is associated with PlexinA4 by 10 min post-treatment, rising to nearly 70% after 20

min. This is in distinct contrast to the colocalization of NRP1 with L1, which falls significantly over the same period, so that by 20 min post-treatment <8% of NRP1 is associated with L1 (Fig. 4*A*). This indicates that PlexinA4 segregates with NRP1 rather than L1 after Sema3A treatment. Consistent with PlexinA4 being trafficked with NRP1, we found that the Sema3A-induced colocalization of NRP1 with PlexinA4 does not occur in TAG1KO growth cones (Fig. 6*A*), and that in wild-type growth cones there is a significant increase in the proportion of TAG1 protein that is colocalized with PlexinA4, as well as with NRP1 (Fig. 6B).

Finally, to determine whether TAG1 is required for the initiation of signals by PlexinA4, we monitored the phosphorylation of Collapsin response mediator protein 2 (CRMP2) using an antibody that recognizes the phosphorylation of CRMP2 at Serine 522, a known readout of Sema3A signaling (Uchida et al., 2005); CRMPs are thought to interact indirectly with the C-terminal region of PlexinAs through direct interactions with MICALs (molecules interacting with CasL), which bind to PlexinAs (Schmidt et al., 2008). Consistent with previous observations (Uchida et al., 2005), in wild-type growth cones we saw a significant increase in the absolute levels of phospho-CRMP (pCRMP) staining 10 min after Sema3A treatment (Fig. 6*C*), coincident with the separation of NRP1 from L1 and its transition into CTxB-enriched intracellular vesicles (Fig. 3*B*). By contrast, this increase does not occur after Sema3A treatment of TAG1KO growth cones (Fig. 6*C*). Together, these data indicate that TAG1-dependent trafficking of NRP1 also affects the trafficking and signaling of PlexinA4, thus accounting for the loss of collapse seen in growth cones lacking TAG1 (Law et al., 2008).

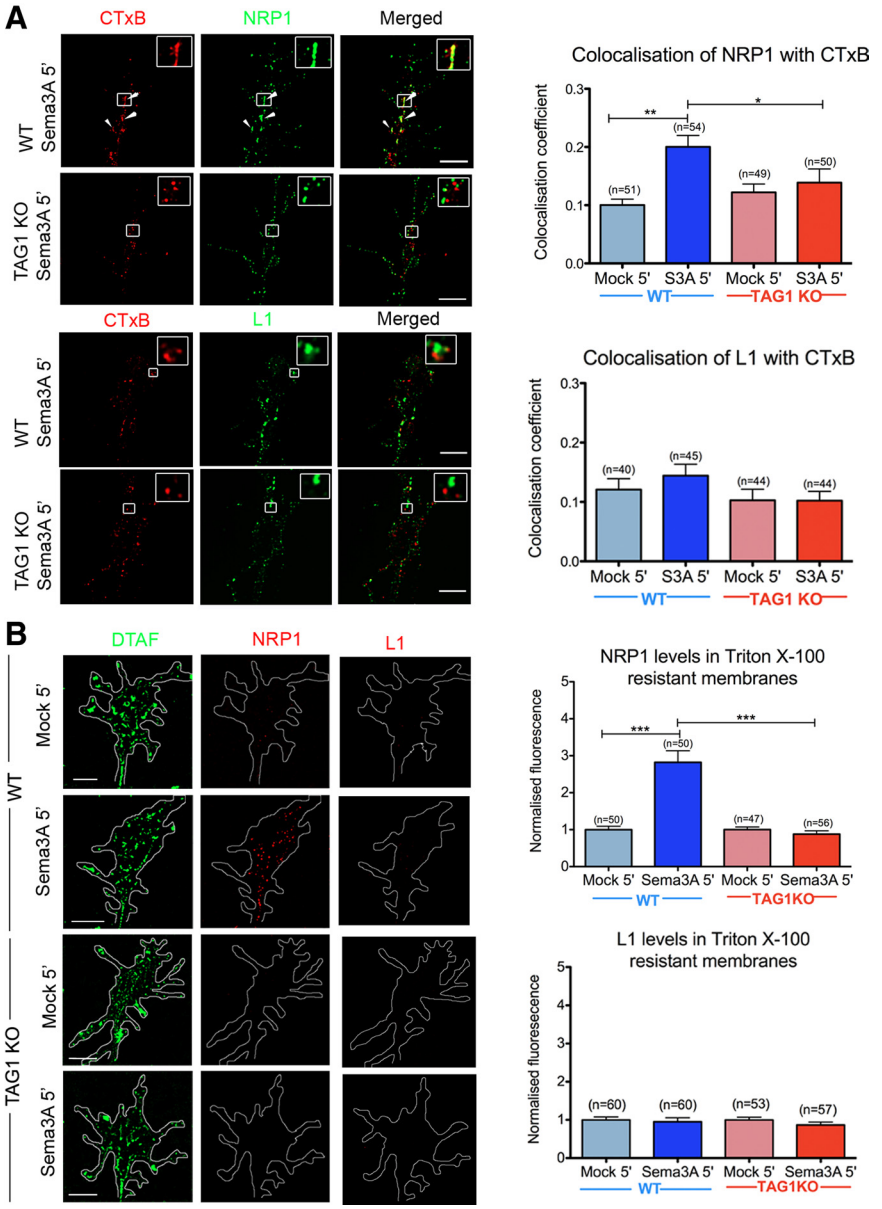

Figure 5. NRP1 localizes to membrane rafts after Sema3A treatment in a TAG1-dependent manner. ***A***, Growth cones treated with Mock or Sema3A medium were labeled for CTxB (red) with either NRP1 or L1 (green). The colocalization of NRP1 with CTxB increased significantly upon Sema3A treatment in WT growth cones (arrowheads, insets) but not in TAG1KO growth cones (one-way ANOVA, $p < 0.001$). On the other hand, L1 did not significantly colocalize with CTxB after Sema3A treatment in WT or TAG1KO growth cones (one-way ANOVA, $p = 0.4503$). ***B***, Detergent-resistant membranes (DRMs) prepared from growth cones treated with Mock or Sema3A-medium and immunolabeled for NRP1 or L1 (red) followed by DTAF (green) for total protein labeling. NRP1 levels detected in the DRMs of WT growth cones treated with Sema3A were significantly higher than those of Mock-treated growth cones. However, this was not observed in DRMs prepared from TAG1 KO growth cones (one-way ANOVA, $p < 0.0001$). No L1 could be detected in DRMs of WT or TAG1KO growth cones under mock or Sema3A conditions (one-way ANOVA, $p = 0.7319$; n = number of growth cones; $^{***}p < 0.001$, $^{**}p < 0.01$, $^{*}p < 0.05$). Scale bar, 5 μm.

Discussion

We showed that TAG1 is a critical component of the Sema3A holoreceptor in DRG neurons that is required for differential trafficking of receptor components into specific intracellular pathways and is essential for signal generation. TAG1 interacts with NRP1 directly and renders the inclusion of L1 in the holoreceptor Sema3A-sensitive; Sema3A binding induces NRP1 and L1 to endocytose together, but intracellularly NRP1 is routed away from L1 into vesicles enriched in CTxB binding sites (Fig. 7*A*), and its association with PlexinA4, the signaling component of the receptor, increases. Concurrently, CRMP2 phosphorylation, an indicator of PlexinA signaling, increases and growth cone collapse is initiated. However, when TAG1 is absent, although NRP1 is still endocytosed with L1, it fails to segregate into CTxB-enriched vesicles, appearing instead to be recycled to the cell surface (Fig. 7*B*); increased association with PlexinA4 does not occur, CRMP2 phosphorylation does not increase, and collapse is attenuated. These observations indicate that TAG1 plays a critical role in the trafficking of semaphorin receptors into specific endocytic pathways and is required to activate PlexinA signaling. Together with previous observations (Castellani et al., 2004, Law et al., 2008), this suggests that adhesion molecule interactions at the cell surface can modulate responses to diffusible signals by altering the endocytic fate of their receptors.

Endocytosis is a key component of many signaling pathways and the endocytic pathway taken by receptors is recognized to

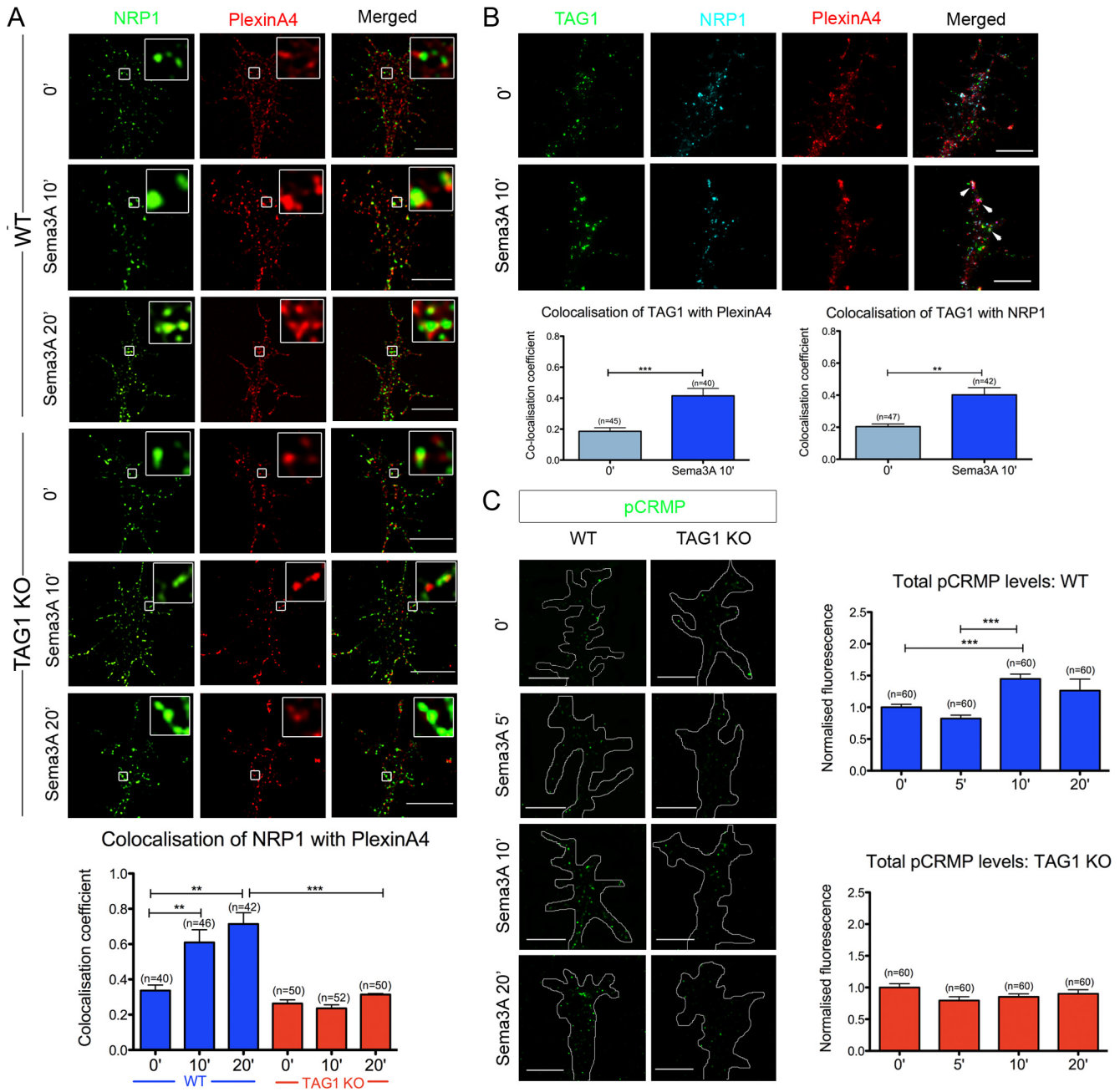

Figure 6. TAG1 is required for the activation of Sema3A signaling. ***A***, Growth cones were fixed, permeabilized, and labeled for NRP1 (green) and PlexinA4 (red) for colocalization analysis. The amount of NRP1 colocalized with PlexinA4 increased after 10 min of Sema3A treatment in WT growth cones and remained high at 20 min (one-way ANOVA, $p < 0.0001$). TAG1KO growth cones failed to show a similar increase in NRP1-PlexinA4 colocalization. ***B***, Sema3A-treated growth cones were processed for immunolabeling for TAG1 (green), NRP1 (cyan), and PlexinA4 (red). The amount of TAG1 colocalized with PlexinA4 (unpaired *t* test, $p < 0.0001$) and NRP1 (unpaired *t* test, $p = 0.0473$) increased after 10 min of Sema3A treatment. ***C***, Sema3A-treated growth cones were processed for immunolabeling with antibody against phosphorylated CRMP (pCRMP) at Serine 522. In WT growth cones, the amount of pCRMP fluorescence increased after 10 min of Sema3A treatment and was still high at 20 min (one-way ANOVA, $p < 0.0001$). TAG1 KO growth cones did not show any such increase in pCRMP fluorescence (one-way ANOVA, $p = 0.1577$). Data are combined values from three independent experiments (*n*, number of growth cones; $^{***}p < 0.001$, $^{**}p < 0.01$, $^{*}p < 0.05$). Scale bar, 5 μm.

affect signaling outcome (Sorkin and von Zastrow, 2009). How pathway selection is controlled remains poorly characterized, especially in neurons where, given their size and complexity, endocytic sorting is crucially important (Von Bartheld and Altick, 2011). Responses mediated by semaphorin-binding neuropilins are known to vary by cell type (Salikhova et al., 2008; Carcea et al., 2010) and in dendrites versus axons (Polleux et al., 2000; Shelly et al., 2011). Responses vary even among neurons expressing similar receptor components (Carcea et al., 2010), but the molecular basis for this is not clear. A key difference between Sema3A responsive and nonresponsive sensory afferents is the expression of the adhesion molecule TAG1 (Law et al., 2008). Here we showed that the GPI-linked protein TAG1 is required to segregate NRP1 from L1 and traffic it to an endosomal subpopulation enriched in lipid rafts, as defined by CTxB binding. GPI-linked proteins are delivered via clathrin-independent endocytosis into GEECs (GPI-enriched endosomal compartments) in a GPI-linkage-dependent manner (Sabharanjak et al., 2002; Mayor and Pagano, 2007). Although the GPI-linked protein Cripto has been shown to localize the precursor of the secreted ligand Nodal to lipid rafts

for processing (Blanchet et al., 2008), we believe this is the first demonstration of an endogenous GPI-linked protein driving sorting of a membrane receptor into raft-enriched intracellular membranes. Moreover, in the absence of TAG1-mediated segregation of NRP1, downstream signaling by Plexin (CRMP2 phosphorylation; Goshima et al., 1995) does not occur, and collapse is attenuated. Although it has been assumed that the segregation of membrane proteins into lipid rafts occurs at the cell surface (Mayor and Pagano, 2007), our results indicate that this can occur intracellularly, consistent with evidence for the existence of endosomal subpopulations specialized for cell signaling (Zoncu et al., 2009).

These and other results suggest that Sema3A binding generates signals at at least three different points in the NRP1 trafficking pathway; Sema3A raises intracellular cGMP and Ca^{2+} levels within 2 min of treatment, which is required for growth cone repulsion (Togashi et al., 2008). Although Ca^{2+}-induced repulsion requires clathrin-dependent endocytosis, Sema3A-induced Ca^{2+} fluxes are endocytosis independent (Tojima et al., 2010), indicating that signaling is initiated at the cell surface (Fig. 7*A*). Endocytosis of NRP1 is dependent on its association with either L1 or PlexinA (Castellani et al., 2004), and L1 is essential for the activation of Focal Adhesion Kinase (FAK), which is required for growth cone collapse and disassembly of focal adhesions (Bechara et al., 2008). FAK is only coprecipitated with L1 when NRP1 is present and this association is enhanced by Sema3A treatment. However, FAK does not associate with PlexinAs, and although PlexinA inhibition prevents collapse in response to Sema3A, focal adhesions still disassemble, indicating that PlexinAs and FAK activate different aspects of the response (Barberis et al., 2004; Bechara et al., 2008). The initial increase in L1/NRP1 association followed by separation and subsequent increase in NRP1/PlexinA4 association, fits with these observations and suggests a model in which the activation of FAK and Plexin are spatially and temporally separated (Fig. 7*A*). The endocytic route taken by L1 after Sema3A treatment appears qualitatively different from that followed during steady-state recycling; after Sema3A, L1 disappears from the cell surface and appears in large intracellular aggregates not seen in the steady state.

The increase of NRP1 association with endocytosed L1 within 5 min of Sema3A treatment is not dependent on TAG1. This appears to conflict with the requirement for TAG1 in the increase in anti-L1 Fab uptake that occurs 10 min after Sema3A addition. However, it is possible that this late increase in L1 endocytosis reflects the general increase in endocytosis that accompanies collapse (Fournier et al., 2000), which only becomes evident around 10 min. Thus, TAG1 may be required in the initiation of collapse rather than for L1 endocytosis per se. CRMP2, through its ability to bind Numb, is known to regulate L1 endocytosis (Nishimura et al., 2003), raising the possibility that L1 uptake is stimulated by feedback from CRMP2 during Sema3A signaling. Enhanced L1 endocytosis in turn may reflect the general disassembly of focal adhesions that accompanies collapse (Bechara et al., 2008).

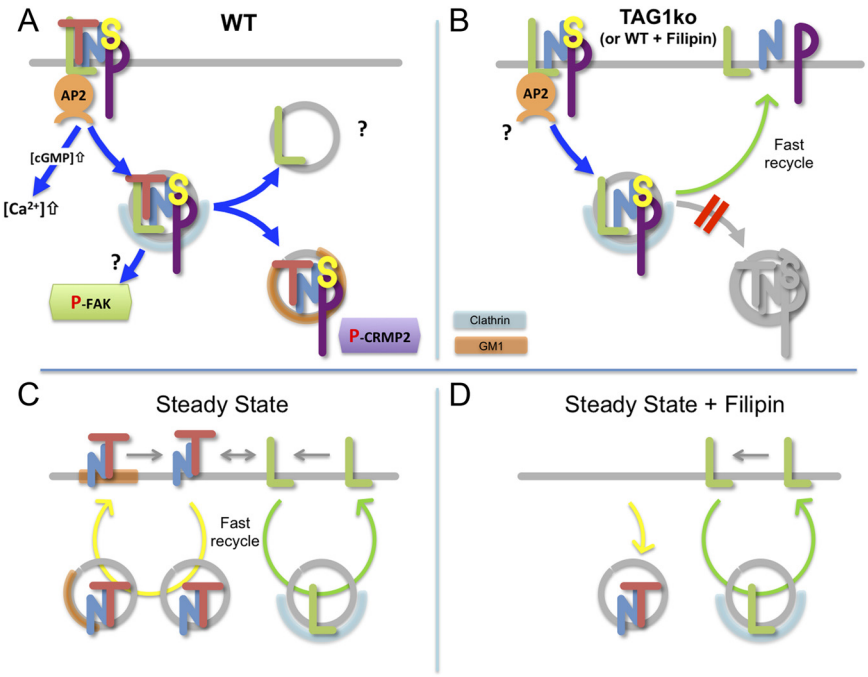

Figure 7. Model of Sema3A receptor endocytosis. ***A***, Upon Sema3A binding, the receptor signals: at the cell surface via cGMP (Togashi et al., 2008; Tojima et al., 2010); after endocytosis via phospho-FAK (Bechara et al., 2008); and after TAG1-dependent separation of NRP1 from L1 via phospho-CRMP2 (this study). ***B***, In the absence of TAG1 (this study) or in the presence of filipin (Guirland et al., 2004), NRP1 fails to enter the raft pathway and instead receptor components are rapidly recycled to the cell surface without affecting the net surface levels. ***C***, ***D***, In the absence of Sema3A, receptor complex components undergo continuous recycling: L1 apparently uses CME (Kamiguchi et al. 1998) and is not sensitive to filipin (data not shown). NRP1, however, disappears from the cell surface after filipin treatment in the steady-state (Fig. 3*A*) suggesting that recycling of NRP1 to the surface, rather than its endocytosis, requires intact rafts. Molecules are represented by letters: L, L1; N, NRP1; P, PlexinA4; S, Sema3A; T, TAG1. Plexin is not included in the steady-state figures (***C***, ***D***) because its disposition is not addressed by our data.

The endocytic route that mediates Sema3A-induced responses remains controversial. Although Sema3A signaling can be blocked by agents that disrupt lipid raft integrity (Guirland et al. 2004; Salikhova et al., 2008; Carcea et al., 2010), an immediate early endocytic response to Sema3A is blocked by dominant-negative mutant endocytic proteins that disrupt CME (Tojima et al., 2010). Although our results are consistent with NRP1 initially entering the cell via CME rather than RME, we cannot rule out that a non-CME pathway such as macropinocytosis is used (Fournier et al., 2000). Since we show that endocytosed NRP1 dissociates from L1 and becomes associated with CTxB-binding membranes, raft-disrupting reagents may inhibit Sema3A signaling (Guirland et al., 2004; Salikhova et al., 2008; Carcea et al., 2010) because they interfere with this latter intracellular step. Nonetheless, RME-inhibiting reagents apparently block Sema-induced endocytosis of Sema3A or NRP1 in some cortical neurons (Carcea et al., 2010) or endothelial cells (Salikhova et al., 2008), whereas CME inhibitors do not. It is possible that different cell types traffic NRP1 differently. However, raft-disrupting agents may appear to block Sema3A-induced endocytosis because they prevent the intracellular diversion of NRP1 into CTxB-binding vesicles and instead receptors are recycled to the surface, leaving net surface levels unaffected (Fig. 7*B*).

We clearly show that NRP1 traffics into CTxB-binding membranes intracellularly. However, we cannot rule out that NRP1 also becomes associated with rafts at the cell surface. Sema3A

treatment of retinal neurons results in rapid NRP1 disappearance from the cell surface, coincident with desensitization, followed by reappearance and resensitization (Piper et al., 2005). This resensitization does not occur if protein synthesis is blocked, even though surface NRP1 levels are restored by recycling. One possibility is that cell surface raft-associated NRP1 represents the pool of recycled but not reactivated receptors, consistent with our observation that L1 does not become raft-associated after Sema3A treatment. The possibility that intact rafts may be required for NRP1 recycling is consistent with our observation that filipin treatment leads to disappearance of NRP1 from the surface of DRG growth cones in the steady state (Figs. 3*A*, 7*C*,*D*), whereas L1 surface levels are not affected (data not shown).

In other cell types, the switch between clathrin-dependent and raft-dependent pathways may nonetheless occur at the cell surface and be regulated differently. For example, in endothelial cells the NRP1 endocytic pathway is apparently determined by the ligand; binding of VEGF leads to CME, whereas binding of Sema3C leads to RME (Salikhova et al., 2008). This may explain why the TAG1 knockout only partially mimics the Sema3A and NRP1 knockout phenotypes (Law et al., 2008); TAG1 may only be required for a subset of Sema responses.

In DRG, however, TAG1 expression clearly correlates with Sema3A responsiveness. Initially, both presumptive proprioceptive and nociceptive axons are repelled by Sema3A (Messersmith et al., 1995; Fu et al., 2000; Pond et al., 2002) and express L1 and TAG1 (Perrin et al., 2001; Law et al., 2008). However, proprioceptive axons lose this sensitivity coincident with TAG1 downregulation and project into the spinal cord (Fu et al., 2000; Pond et al., 2002; Law et al., 2008). TAG1 loss leads to premature nociceptive entry into the dorsal horn (Law et al., 2008), mimicking the effects of loss of NRP1 (Gu et al., 2003). Thus, in DRG neurons TAG1 determines the outcome of Sema3A signaling by altering the intracellular trafficking of the core receptor components. That such a role is assumed by an adhesion molecule suggests this is a mechanism by which growth cones modulate their responses to guidance cues according to cellular context, an idea strongly supported by the observation that cross-linking of the receptor complex with L1 inhibits Sema3A-induced growth cone collapse (Castellani et al. 2000, 2002).

References

Barberis D, Artigiani S, Casazza A, Corso S, Giordano S, Love CA, Jones EY, Comoglio PM, Tamagnone L (2004) Plexin signaling hampers integrin-based adhesion, leading to Rho-kinase independent cell rounding, and inhibiting lamellipodia extension and cell motility. FASEB J 18:592–594.

Bechara A, Nawabi H, Moret F, Yaron A, Weaver E, Bozon M, Abouzid K, Guan JL, Tessier-Lavigne M, Lemmon V, Castellani V (2008) FAK-MAPK-dependent adhesion disassembly downstream of L1 contributes to semaphorin3A-induced collapse. EMBO J 27:1549–1562.

Blanchet MH, Le Good JA, Oorschot V, Baflast S, Minchiotti G, Klumperman J, Constam DB (2008) Cripto localizes Nodal at the limiting membrane of early endosomes. Sci Signal 1:ra13.

Buchstaller A, Kunz S, Berger P, Kunz B, Ziegler U, Rader C, Sonderegger P (1996) Cell adhesion molecules NgCAM and axonin-1 form heterodimers in the neuronal membrane and cooperate in neurite outgrowth promotion. J Cell Biol 135:1593–1607.

Carcea I, Ma'ayan A, Mesias R, Sepulveda B, Salton SR, Benson DL (2010) Flotillin-mediated endocytic events dictate cell type-specific responses to semaphorin 3A. J Neurosci 30:15317–15329.

Castellani V, Chédotal A, Schachner M, Faivre-Sarrailh C, Rougon G (2000) Analysis of the L1-deficient mouse phenotype reveals cross-talk between Sema3A and L1 signaling pathways in axonal guidance. Neuron 27:237–249.

Castellani V, De Angelis E, Kenwrick S, Rougon G (2002) Cis and trans interactions of L1 with neuropilin-1 control axonal responses to semaphorin 3A. EMBO J 21:6348–6357.

Castellani V, Falk J, Rougon G (2004) Semaphorin3A-induced receptor endocytosis during axon guidance responses is mediated by L1 CAM. Mol Cell Neurosci 26:89–100.

Collinet C, Stöter M, Bradshaw CR, Samusik N, Rink JC, Kenski D, Habermann B, Buchholz F, Henschel R, Mueller MS, Nagel WE, Fava E, Kalaidzidis Y, Zerial M (2010) Systems survey of endocytosis by multiparametric image analysis. Nature 464:243–249.

Conner SD, Schmid SL (2003) Regulated portals of entry into the cell. Nature 422:37–44.

Di Guglielmo GM, Le Roy C, Goodfellow AF, Wrana JL (2003) Distinct endocytic pathways regulate TGF-beta receptor signalling and turnover. Nat Cell Biol 5:410–421.

Fournier AE, Nakamura F, Kawamoto S, Goshima Y, Kalb RG, Strittmatter SM (2000) Semaphorin3A enhances endocytosis at sites of receptor-F-actin colocalization during growth cone collapse. J Cell Biol 149:411–422.

Fu SY, Sharma K, Luo Y, Raper JA, Frank E (2000) SEMA3A regulates developing sensory projections in the chicken spinal cord. J Neurobiol 45:227–236.

Goshima Y, Nakamura F, Strittmatter P, Strittmatter SM (1995) Collapsin-induced growth cone collapse mediated by an intracellular protein related to UNC-33. Nature 376:509–514.

Gu C, Rodriguez ER, Reimert DV, Shu T, Fritzsch B, Richards LJ, Kolodkin AL, Ginty DD (2003) Neuropilin-1 conveys semaphorin and VEGF signaling during neural and cardiovascular development. Dev Cell 5:45–57.

Guirland C, Suzuki S, Kojima M, Lu B, Zheng JQ (2004) Lipid rafts mediate chemotropic guidance of nerve growth cones. Neuron 42:51–62.

Harder T, Scheiffele P, Verkade P, Simons K (1998) Lipid domain structure of the plasma membrane revealed by patching of membrane components. J Cell Biol 141:929–942.

Itoh K, Cheng L, Kamei Y, Fushiki S, Kamiguchi H, Gutwein P, Stoeck A, Arnold B, Altevogt P, Lemmon V (2004) Brain development in mice lacking L1–L1 homophilic adhesion. J Cell Biol 165:145–154.

Ivanov AI (2008) Pharmacological inhibition of endocytic pathways: is it specific enough to be useful? Methods Mol Biol 440:15–33.

Kamiguchi H, Lemmon V (2000) Recycling of the cell adhesion molecule L1 in axonal growth cones. J Neurosci 20:3676–3686.

Kamiguchi H, Yoshihara F (2001) The role of endocytic l1 trafficking in polarized adhesion and migration of nerve growth cones. J Neurosci 21:9194–9203.

Kamiguchi H, Long KE, Pendergast M, Schaefer AW, Rapoport I, Kirchhausen T, Lemmon V (1998) The neural cell adhesion molecule L1 interacts with the AP-2 adaptor and is endocytosed via the clathrin-mediated pathway. J Neurosci 18:5311–5321.

Kasahara K, Watanabe K, Kozutsumi Y, Oohira A, Yamamoto T, Sanai Y (2002) Association of GPI-anchored protein TAG-1 with src-family kinase Lyn in lipid rafts of cerebellar granule cells. Neurochem Res 27:823–829.

Kawauchi T, Sekine K, Shikanai M, Chihama K, Tomita K, Kubo K, Nakajima K, Nabeshima Y, Hoshino M (2010) Rab GTPases-dependent endocytic pathways regulate neuronal migration and maturation through N-cadherin trafficking. Neuron 67:588–602.

Kolodkin AL, Levengood DV, Rowe EG, Tai YT, Giger RJ, Ginty DD (1997) Neuropilin is a semaphorin III receptor. Cell 90:753–762.

Law CO, Kirby RJ, Aghamohammadzadeh S, Furley AJ (2008) The neural adhesion molecule TAG-1 modulates responses of sensory axons to diffusible guidance signals. Development 135:2361–2371.

Lee JA, Gao FB (2008) ESCRT, autophagy, and frontotemporal dementia. BMB Rep 41:827–832.

Letourneau PC (1983) Differences in the organization of actin in the growth cones compared with the neurites of cultured neurons from chick embryos. J Cell Biol 97:963–973.

Loberto N, Prioni S, Prinetti A, Ottico E, Chigorno V, Karagogeos D, Sonnino S (2003) The adhesion protein TAG-1 has a ganglioside environment in the sphingolipid-enriched membrane domains of neuronal cells in culture. J Neurochem 85:224–233.

Lowe M (2005) Structure and function of the Lowe syndrome protein OCRL1. Traffic 6:711–719.

Malhotra JD, Tsiotra P, Karagogeos D, Hortsch M (1998) Cis-activation of L1-mediated ankyrin recruitment by TAG-1 homophilic cell adhesion. J Biol Chem 273:33354–33359.

Marquardt T, Shirasaki R, Ghosh S, Andrews SE, Carter N, Hunter T, Pfaff SL (2005) Coexpressed EphA receptors and ephrin-A ligands mediate opposing actions on growth cone navigation from distinct membrane domains. Cell 121:127–139.

Mayor S, Pagano RE (2007) Pathways of clathrin-independent endocytosis. Nat Rev Mol Cell Biol 8:603–612.

Mayor S, Sabharanjak S, Maxfield FR (1998) Cholesterol-dependent retention of GPI-anchored proteins in endosomes. EMBO J 17:4626–4638.

Mechtersheimer S, Gutwein P, Agmon-Levin N, Stoeck A, Oleszewski M, Riedle S, Postina R, Fahrenholz F, Fogel M, Lemmon V, Altevogt P (2001) Ectodomain shedding of L1 adhesion molecule promotes cell migration by autocrine binding to integrins. J Cell Biol 155:661–673.

Messersmith EK, Leonardo ED, Shatz CJ, Tessier-Lavigne M, Goodman CS, Kolodkin AL (1995) Semaphorin III can function as a selective chemorepellent to pattern sensory projections in the spinal cord. Neuron 14:949–959.

Moretti S, Procopio A, Lazzarini R, Rippo MR, Testa R, Marra M, Tamagnone L, Catalano A (2008) Semaphorin3A signaling controls Fas (CD95)-mediated apoptosis by promoting Fas translocation into lipid rafts. Blood 111:2290–2299.

Nakamura Y, Lee S, Haddox CL, Weaver EJ, Lemmon VP (2010) Role of the cytoplasmic domain of the L1 cell adhesion molecule in brain development. J Comp Neurol 518:1113–1132.

Nishimura T, Fukata Y, Kato K, Yamaguchi T, Matsuura Y, Kamiguchi H, Kaibuchi K (2003) CRMP-2 regulates polarized Numb-mediated endocytosis for axon growth. Nat Cell Biol 5:819–826.

Pellet-Many C, Frankel P, Jia H, Zachary I (2008) Neuropilins: structure, function and role in disease. Biochem J 411:211–226.

Perrin FE, Rathjen F, Stoeckli E (2001) Distinct subpopulations of sensory afferents require F11 or axonin-1 for growth to their target layers within the spinal cord of the chick. Neuron 30:707–723.

Piper M, Salih S, Weinl C, Holt CE, Harris WA (2005) Endocytosis-dependent desensitization and protein synthesis-dependent resensitization in retinal growth cone adaptation. Nat Neurosci 8:179–186.

Poliak S, Salomon D, Elhanany H, Sabanay H, Kiernan B, Pevny L, Stewart CL, Xu X, Chiu SY, Shrager P, Furley AJW, Peles E (2003) Juxtaparanodal clustering of *Shaker*-like K^+ channels in myelinated axons depends on Caspr2 and TAG-1. J Cell Biol 162:1149–1160.

Polleux F, Morrow T, Ghosh A (2000) Semaphorin 3A is a chemoattractant for cortical apical dendrites. Nature 404:567–573.

Pond A, Roche FK, Letourneau PC (2002) Temporal regulation of neuropilin-1 expression and sensitivity to semaphorin 3A in NGF- and NT3-responsive chick sensory neurons. J Neurobiol 51:43–53.

Püschel AW, Adams RH, Betz H (1996) The sensory innervation of the mouse spinal cord may be patterned by differential expression of and differential responsiveness to semaphorins. Mol Cell Neurosci 7:419–431.

Rader C, Kunz B, Lierheimer R, Giger RJ, Berger P, Tittmann P, Gross H, Sonderegger P (1996) Implications for the domain arrangement of axonin-1 derived from the mapping of its NgCAM binding site. EMBO J 15:2056–2068.

Sabharanjak S, Sharma P, Parton RG, Mayor S (2002) GPI-anchored proteins are delivered to recycling endosomes via a distinct cdc42-regulated, clathrin-independent pinocytic pathway. Dev Cell 2:411–423.

Salikhova A, Wang L, Lanahan AA, Liu M, Simons M, Leenders WP, Mukhopadhyay D, Horowitz A (2008) Vascular endothelial growth factor and semaphorin induce neuropilin-1 endocytosis via separate pathways. Circ Res 103:e71–e79.

Schaefer AW, Kamei Y, Kamiguchi H, Wong EV, Rapoport I, Kirchhausen T, Beach CM, Landreth G, Lemmon SK, Lemmon V (2002) L1 endocytosis is controlled by a phosphorylation-dephosphorylation cycle stimulated by outside-in signaling by L1. J Cell Biol 157:1223–1232.

Schmidt EF, Shim SO, Strittmatter SM (2008) Release of MICAL autoinhibition by semaphorin-plexin signaling promotes interaction with collapsin response mediator protein. J Neurosci 28:2287–2297.

Sheen VL, Ganesh VS, Topcu M, Sebire G, Bodell A, Hill RS, Grant PE, Shugart YY, Imitola J, Khoury SJ, Guerrini R, Walsh CA (2004) Mutations in ARFGEF2 implicate vesicle trafficking in neural progenitor proliferation and migration in the human cerebral cortex. Nat Genet 36:69–76.

Shelly M, Cancedda L, Lim BK, Popescu AT, Cheng PL, Gao H, Poo MM (2011) Semaphorin3A regulates neuronal polarization by suppressing axon formation and promoting dendrite growth. Neuron 71:433–446.

Sorkin A, von Zastrow M (2009) Endocytosis and signalling: intertwining molecular networks. Nat Rev Mol Cell Biol 10:609–622.

Suto F, Ito K, Uemura M, Shimizu M, Shinkawa Y, Sanbo M, Shinoda T, Tsuboi M, Takashima S, Yagi T, Fujisawa H (2005) Plexin-a4 mediates axon-repulsive activities of both secreted and transmembrane semaphorins and plays roles in nerve fiber guidance. J Neurosci 25:3628–3637.

Takahashi T, Fournier A, Nakamura F, Wang LH, Murakami Y, Kalb RG, Fujisawa H, Strittmatter SM (1999) Plexin-neuropilin-1 complexes form functional semaphorin-3A receptors. Cell 99:59–69.

Togashi K, von Schimmelmann MJ, Nishiyama M, Lim CS, Yoshida N, Yun B, Molday RS, Goshima Y, Hong K (2008) Cyclic GMP-gated CNG channels function in Sema3A-induced growth cone repulsion. Neuron 58:694–707.

Tojima T, Itofusa R, Kamiguchi H (2010) Asymmetric clathrin-mediated endocytosis drives repulsive growth cone guidance. Neuron 66:370–377.

Tran TS, Kolodkin AL, Bharadwaj R (2007) Semaphorin regulation of cellular morphology. Annu Rev Cell Dev Biol 23:263–292.

Uchida Y, Ohshima T, Sasaki Y, Suzuki H, Yanai S, Yamashita N, Nakamura F, Takei K, Ihara Y, Mikoshiba K, Kolattukudy P, Honnorat J, Goshima Y (2005) Semaphorin3A signalling is mediated via sequential Cdk5 and GSK3beta phosphorylation of CRMP2: implication of common phosphorylating mechanism underlying axon guidance and Alzheimer's disease. Genes Cells 10:165–179.

Von Bartheld CS, Altick AL (2011) Multivesicular bodies in neurons: distribution, protein content, and trafficking functions. Prog Neurobiol 93:313–340.

Yaron A, Huang PH, Cheng HJ, Tessier-Lavigne M (2005) Differential requirement for Plexin-A3 and -A4 in mediating responses of sensory and sympathetic neurons to distinct class 3 Semaphorins. Neuron 45:513–523.

Zanata SM, Hovatta I, Rohm B, Püschel AW (2002) Antagonistic effects of Rnd1 and RhoD GTPases regulate receptor activity in Semaphorin 3A-induced cytoskeletal collapse. J Neurosci 22:471–477.

Zoncu R, Perera RM, Balkin DM, Pirruccello M, Toomre D, De Camilli P (2009) A phosphoinositide switch controls the maturation and signaling properties of APPL endosomes. Cell 136:1110–1121.